Published in final edited form as:
Cytoskeleton (Hoboken). 2010 January ; 67(1): 32–42. doi:10.1002/cm.20419.

Myosin IIB isoform plays an essential role in the formation of two distinct types of macropinosomes

Jun Jiang, **Adrianne L. Kolpak**, and **Zheng-Zheng Bao**
Department of Medicine and Cell Biology, Program in Neuroscience, University of Massachusetts Medical School, Worcester, Massachusetts 01605

Abstract

The function and mechanism of macropinocytosis in cells outside of the immune system remain poorly understood. We used a neuroblastoma cell line, Neuro-2a, to study macropinocytosis in neuronal cells. We found phorbol 12-myristate 13-acetate (PMA) and insulin-like growth factor 1 (IGF-1) induced two dinstinct types of macropinocytosis in the Neuro-2a cells. IGF-1-induced macropinocytosis occurs mostly around the cell bodies and requires phosphoinositide 3-kinase (PI3K), while PMA-induced macropinocytosis occurs predominantly in the neurites and is independent of PI3K. Both types of macropinocytosis were inhibited by a specific inhibitor of non-muscle myosin II, blebbistatin. siRNA knock-down of nonmuscle myosin II isoforms, -IIA and –IIB, resulted in opposite effects on macropinocytosis induced by PMA or IGF. Myosin IIA knock-down significantly increased, whereas myosin IIB knock-down significantly decreased, macropinocytosis with correlating changes in membrane ruffle formation.

Keywords

myosin IIB; myosin IIA; macropinocytosis

INTRODUCTION

Macropinocytosis is a type of fluid-phase endocytosis characterized by its independence of clathrin which results in relatively large sizes of vesicles ranging from 0.2 to 1 μm (Jones 2007; Swanson 2008; Swanson and Watts 1995). Macropinocytosis occurs predominantly in macrophages, dendritic cells and *Dictyostelium* cells. In *Dictyostelium*, macropinocytosis serves the purposes of fluid and nutrient uptake (Maniak 2001). Constitutive macropinocytosis in dendritic cells internalizes large quantities of fluid-phase solutes as part of the sentinel function and antigen presentation (Nobes and Marsh 2000; Norbury 2006; Norbury et al. 1995). In other types of cells, macropinocytosis occurs at a low spontaneous rate but is rapidly induced in response to growth factors including platelet-derived growth factor (PDGF) and epidermal growth factor (EGF) (Hewlett et al. 1994; West et al. 1989).

The biological function of growth factor-induced macropinocytosis remains poorly understood. Unlike constitutive macropinocytosis in macrophages and dendritic cells (Racoosin and Swanson 1993), macropinocytosis transiently induced by growth factors have been shown not to deliver their content to the lysosomal pathway for degradation, rather recycled back to the cell surface (Hewlett et al. 1994). Recently, macropinocytosis has been recognized as one of the pathways exploited by the pathogen to gain entry into host cells (Meier and Greber 2004; Pelkmans and Helenius 2003; Sieczkarski and Whittaker 2002).

*Author for correspondence: zheng.bao@umassmed.edu, Phone: 508-856-3202, FAX: 508-856-6176.

Adenovirus type 2 enters the cell through clathrin-mediated endocytosis and can additionally trigger macropinocytosis and endosomal leakage (Meier et al. 2002).

Macropinocytosis is characterized as independent of the function of clathrin and caveolin (Conner and Schmid 2003). Instead, macropinocytosis is intimately linked with membrane ruffling. Ruffles are sheet-like extensions of the cell surface resulting from assembly of actin filaments beneath the plasma membrane. Although not all membrane ruffles lead to formation of macropinosomes, some fold back to the plasma membrane and close into intracellular vesicles. Phosphoinositide 3-kinase (PI3K) and P21-activated kinase (PAK) are important regulators of macropinocytosis (Amyere et al. 2000; Anton et al. 2003; Araki et al. 1996; D'Angelo et al. 2007; Dharmawardhane et al. 2000; Ellerbroek et al. 2004; Fiorentini et al. 2001; Hall 1992; Kruth et al. 2005; Rupper et al. 2001; West et al. 2000). Inhibitors of PI3K inhibit both membrane ruffling and macropinocytosis induced by insulin in epidermoid carcinoma KB cells (Kotani et al. 1995), but only inhibit macropinosome closure not membrane ruffles in EGF-stimulated epidermal A431 cells (Araki et al. 2007). PAK1 activity enhances macropinocytosis but not clathrin-mediated endocytosis, and modulates pinocytic vesicle cycling (Dharmawardhane et al. 2000).

The actin-based motor proteins, myosins, have been shown to be required for macropinocytosis in *Dictyostelium* (Novak et al. 1995). Double mutants of class I myosin genes, myosin IA^{-}/B^{-} or myosin IB^{-}/C^{-} showed a reduction in fluid phase and membrane uptake without affecting phagocytosis. In macrophages, an inhibitor to myosin light chain kinase (MLCK), ML-7, was used to show that myosin II inhibition attenuated macropinocytosis by decreasing ruffle movement (Araki et al. 2003). However, the role of nonmuscle myosin II isoforms has yet to be examined. Class II myosins are composed of two heavy chains, two essential light chains and two regulatory light chains (Conti and Adelstein 2008; Landsverk and Epstein 2005). Three non-muscle myosin II isoforms have been characterized composed of myosin IIA-C heavy chain isoforms encoded by the genes *MYH9*, *MYH10* and *MYH14*, respectively. Despite high homology in amino acid sequence (Golomb et al. 2004), myosin IIA and myosin IIB have been shown to have different ATPase activity, subcellular localization (Bresnick 1999) and have isoform-specific roles in cell migration (Betapudi et al. 2006; Even-Ram et al. 2007; Swailes et al. 2006; Vicente-Manzanares et al. 2007), cytokinesis (Bao et al. 2007) and neurite growth (Wylie and Chantler 2001).

To further characterize the regulation and function of macropinocytosis in neuronal cells, we used a neuroblastoma cell line, Neuro-2a, as a model system. Here we show that phorbol 12-myristate 13-acetate (PMA) and insulin-like growth factor 1 (IGF-1) induced macropinocytosis in the Neuro-2a cells as indicated by uptake of macropinocytosis tracers including dextran and horseradish peroxidase. Myosin IIB relocalizes in response to PMA and IGF-1, to the areas where the dextran-positive vesicles form. siRNA knock-down of myosin IIB significantly decreased whereas knockdown of myosin IIA significantly increased macropinocytosis and membrane ruffles in response to PMA and IGF-1. Double knock-down of myosin IIA and IIB exhibited similar effects on macropinocytosis and membrane ruffles as myosin IIB single knockdown. These results indicate that Neuro-2a can be used as a system to study macropinocytosis in neuronal cells and nonmuscle myosin II has isoform-specific effects on macropinocytosis.

RESULTS

As the function of macropinocytosis in cells other than macrophages and neutrophils remains elusive, we used a neuroblastoma cell line, Neuro-2a, as a model system. Neuro-2a has the advantage of easy transfectability compared to other neuronal cell lines, and can be

differentiated to grow neurites. As phorbol 12-myristate 13-acetate (PMA) is known to induce macropinocytosis in a variety of cell types including macrophages, neurtrophils, fibroblasts, and epithelial cells (Aballay et al. 1999; Beron et al. 1997; Kruth et al. 2002; Langweiler and Davis 1988; Phaire-Washington et al. 1980; Sato et al. 1996), Neuro-2a cells were co-incubated with PMA and a fluid-phase endocytosis tracer FITC-dextran for 2 minutes. Brief pulse labeling allows labeling of the newly formed endocytic vesicles rather than the vesicles further downstream. After labeling, cells were rinsed, fixed and the uptake of FITC-dextran was observed by fluorescence microscopy.

The dextran-positive vesicles were relatively large with an average diameter of 0.49 μm (0.22–1.16 μm) (Fig. 1A), in the range of sizes for macropinosomes. The dextran+ (dex+) vesicles appeared to correspond to the reverse shadowcast vesicles visible under differential interference contrast (DIC) microscopy, and were largely localized in the areas with actin-rich membrane ruffles (Fig. 1A, D). PMA treatment significantly increased the percentage of cells undergoing macropinocytosis as indicated by dextran uptake (Fig. 1A, B). In the control cells without the treatment of PMA, 10.5±2.1% of the cells were labeled by dextran. 3 minute pretreatment of PMA followed by 2 minute labeling with dextran and PMA resulted in 38.1±6.3% of the total number of cells containing dex+ macropinosomes ($p<0.05$). Majority of the dex+ vesicles (81.5%, n=905 vesicles) stimulated by PMA were found in the neurites and processes rather than the cell bodies.

To study the role of myosin in dextran uptake in Neuro-2a cells, we treated the cells with a pharmacological inhibitor, blebbistatin, to inhibit myosin II activity. Blebbistatin was found to inhibit the PMA-induced macropinocytosis effectively (15.7±1.3% dextran uptake rate in the blebbistatin and PMA-treated samples vs. 38.1±6.3% dextran uptake rate in PMA-treated samples, Fig. 1C). We verified the results by using horseradish peroxidase (HRP), another commonly used fluid-phase endocytosis marker. A chemiluminescent substrate, the SuperSignal ELISA Pico Chemiluminescent substrate (Thermo Scientific), instead of the conventional chromogenic substrate of HRP, was used to improve the sensitivity of the assay. The chemiluminescent substrate of HRP was found to yield reliable results with much higher sensitivity than the conventional chromogenic substrates. Incubation of cells at 4°C reduced uptake by 71.3±2.2%, suggesting that HRP was taken into cells mainly via endocytosis. Consistent with the dextran experiments, HRP uptake induced by PMA was significantly reduced by co-incubation with cytochalasin D (Fig. 1E). HRP uptake experiments thus confirmed that the PMA treatment significantly increased macropinocytosis in the Neuro-2a cells, which was inhibited by co-incubation with blebbistatin (Fig. 1D).

Non-muscle myosin II proteins consist of three isoforms, myosin IIAs,-IIB, and -IIC, each with distinct heavy chain subunits encoded by genes *MYH9*, *MYH10* and *MYH14*, respectively. To identify which myosin II isoform may be involved in macropinocytosis, we immunostained the FITC-dextran-labeled cells with antibodies specific to myosin IIA and IIB heavy chains. As shown in Fig. 2A, in the control untreated cells, myosin IIA is distributed throughout the cells and concentrated in some of the tips (growth cones) of the neurites, whereas myosin IIB localization appears variable from cell to cell but generally restricted to the cell body (Fig. 2A). After treatment with PMA for 5 minutes, myosin IIA is redistributed mostly to cell bodies and away from the tips of the neurites (Fig. 2B). In contrast, localization of myosin IIB appears to shift to the tips of the neurites in close proximity to the dex+ vesicles (Fig. 2B).

To study the role of myosin II isoforms in macropinocytosis in the Neuro-2a cells, *myosin IIA* and *-IIB heavy chain* (*MYH9*, *MYH10*) genes were specifically knocked down by transfection of siRNAs. Two sets of siRNAs were designed to target different regions of

myosin IIA and *myosin IIB heavy chain* (*MYH9*, *MYH10*) genes, respectively. As shown in Fig. 3A, C, myosin IIA protein expression was effectively reduced by transfection of either IIA1 or IIA2 siRNA, but unaltered in the cells transfected with the non-silencing siRNA (CTL) or siRNAs targeting myosin IIB (IIB1 or IIB2). More than half of the cells (~70%) showed substantial reduction of myosin IIA protein level in the IIA1 KD- or IIA2 KD-transfected cells by antibody staining (Fig. 3A). Similar specific knockdown effects were observed for myosin IIB by using siRNAs targeting two different regions of *myosin IIB heavy chain*, IIB1 and IIB2 (Fig. 3B, C). Knockdown of one myosin II isoform did not appear to affect the expression of the other isoform, confirming the specificity of knockdown (Fig. 3A–C).

Next, PMA-induced macropinocytosis was analyzed in the myosin IIA- or myosin IIB-knock down (KD) cells. Two sets of siRNAs targeting myosin IIA or myosin IIB or the non-silencing siRNA CTL were transfected into the Neuro-2a cells. After 72 hours, cells were pretreated with PMA for 3 min, followed by FITC-dextran labeling for 2 minutes. The percentages of cells containing dex+ macropinosomes were scored. In response to PMA treatment, the CTL siRNA-transfected cells showed a similar level of dextran uptake as the untransfected WT cells (data not shown). However, both the IIB1 KD and IIB2 KD cells exhibited a significant decrease in dex+ macropinosomes induced by PMA (Fig. 4A,B, $p<0.01$). In contrast, IIA1 KD- or IIA2 KD-transfected cells showed a significant increase in the percentages of cells that undergo dextran uptake upon the treatment of PMA (Fig. 4A, B, $p<0.01$). The changes in macropinocytosis in the siRNA knockdown cells were also verified by quantification of HRP uptake induced by PMA (Fig. 4C). Similar to dextran labeling experiments, knockdown of myosin IIB resulted in a significant decrease whereas knockdown of myosin IIA resulted in a significant increase of HRP uptake compared to the cells transfected with nonsilencing control.

To test whether myosin IIB is required for macropinocytosis induced by other factors, we tested a number of growth factors including insulin-like growth factor-I (IGF-I), nerve growth factor (NGF) and epidermal growth factor (EGF). Whereas neither NGF nor EGF induced macropinocytosis in Neuro-2a cells possibly due to a lack of appropriate receptors, IGF-1 rapidly stimulated macropinocytosis in the Neuro-2a cells (Fig. 5A). Different from the dex+ vesicles induced by PMA, IGF-1-induced dex+ vesicles tended to localize around the cell bodies rather than in the neurites or processes of the cells (84.4% around the cell body, n=1040 vesicles). To characterize these vesicles further, we used known inhibitors of macropinocytosis, including LY294002 for inhibition of phosphoinositide 3 kinase (PI3K) (Araki et al. 1996), 5-(N-ethyl-N-isopropyl) amirolide (EIPA) for inhibition of Na^+/H^+ exchanger (NHE) (Meier et al. 2002), and IPA-3 for inhibition of P21-activated kinase (PAK) (Deacon et al. 2008;Dharmawardhane et al. 2000). EIPA and IPA-3 effectively inhibited macropinocytosis induced by PMA or IGF-1. However, inhibition of PI3K only inhibited IGF-1-induced macropinocytosis but not the PMA-induced macropinocytosis (Fig. 5A, B). These results suggest that macropinocytosis induced by PMA and IGF-1 share common features but also have distinct characteristics.

Similar to the PMA-induced macropinocytosis, IGF-1-induced dextran uptake was also significantly inhibited by co-incubation with blebbistatin. In response to IGF-1, 23.9±4.0% blebbistatin-treated cells were dex+, compared to 48.8±0.6% of the vehicle-treated cells ($p<0.01$). A comparison of dex+ vesicles with the localization of myosin II proteins was carried out by immunostaining using the antibodies specific for myosin II isoforms on the samples that had been incubated with IGF-1 and FITC-dextran. As shown in Fig. 6A, myosin IIB appeared to localize in the areas of membrane ruffles around the cell body induced by IGF-1, whereas myosin IIA was concentrated around the nucleus and on the neurite with some weak staining around the dex+ vesicles. The effects of myosin IIA and

IIB knockdown on IGF-1-induced macropinocytosis were also analyzed. Chemiluminescence substrate was used to measure the amount of HRP uptake. As shown in Fig. 6B, compared to the non-silencing control-transfected cells (CTL), myosin IIB KD cells showed a decrease whereas myosin IIA KD cells showed an increase in HRP uptake. These results demonstrate that myosin IIA and IIB knockdown had similar effects on macropinocytosis induced by IGF-1 as that by PMA. To further analyze the roles of myosin IIA and IIB in macropinocytosis, we performed double knockdown by co-transfecting the IIA1 and IIB1 siRNAs into the Neuro-2a cells. Interestingly, the double knockdown cells showed a similar decrease of macropinocytosis induced by PMA or IGF-1, similarly as in the myosin IIB single knockdown cells (Fig. 4C and Fig. 6B).

The effects of myosin II isoforms on macropinocytosis were further analyzed by examination of membrane ruffle formation in Neuro-2a cells in response to PMA or IGF-1. Both PMA and IGF-1 treatment increased membrane ruffles as shown by phalloidin staining in the Neuro-2a cells (Fig. 7A). The localization of membrane ruffles stimulated by PMA or IGF-1 corresponded to the sites of macropinocytosis induced by these factors. PMA-induced membrane ruffles tended to be wavy, at the cell edge, and on the neurites/processes. IGF-1-induced membrane ruffles tended to be circular, away from the edge of cell, and concentrated on the cell bodies (Fig. 7A). siRNA knockdown of myosin IIA significantly increased, whereas knockdown of myosin IIB significantly decreased, the percentage of cells containing ruffles induced by PMA and IGF-1 (Fig. 7B). Myosin IIB knockdown cells appeared to have more prominent filopodial staining (Fig. 7A). The amount of membrane ruffles also appeared increased in each cell with myosin IIA knockdown, but the type and the localization of the ruffles remain appropriate for the inducer (Fig. 7A, B). These results demonstrate that myosin IIA and IIB play important roles in the formation of membrane ruffles preceding macropinocytosis.

DISCUSSION

Macropinocytosis is constitutive in certain cell types such as dendritic cells, but for most other types of cells, is an induced response to growth factor signaling (Jones 2007). Increasing evidence suggests that macropinocytosis plays an important role for dendritic cells to sample large quantities of exogenous solute as part of their sentinel functions. However, functions and mechanisms of macropinocytosis in other cell types remain elusive. Here, we show that macropinocytosis can be induced in a neuroblastoma cell line, Neuro-2a cells, by phorbol ester and IGF-1. Interestingly, PMA and IGF-1 stimulate macropinocytosis in different locations in the cell and with different requirement of PI3K activity. In addition, we show that non-muscle myosin II isoforms, myosin IIA and IIB, have opposite effects on macropinocytosis in Neuro-2a cells. siRNA knockdown of myosin IIA significantly increases, whereas myosin IIB knockdown significantly decreases, macropinocytosis. Furthermore, we show that the effects of myosin II isoforms on macropinocytosis are likely through their effects on membrane ruffle formation in response to PMA or IGF-1.

Based on their relatively large sizes (>0.2 um in diameter), and the close association with membrane ruffles, the dex+ vesicles induced by PMA and IGF-1 fit into the category of macropinosomes. This was further supported by the results that dextran uptake induced by PMA or IGF-1 was inhibited by treatment of known macropinocytosis inhibitors including EIPA (NHE inhibitor) and IPA-3 (PAK1 inhibitor). However, these dex+ vesicles also have distinct characteristics: the PMA-induced dex+ vesicles are localized in the neurites and processes whereas the IGF-1-induced dex+ vesicles are concentrated around the cell bodies. The PMA-induced macropinocytosis also does not require PI3K signaling, unlike most types of macropinocytosis previously reported. However, it has been shown recently that internalization of the urokinase receptor (uPAR) is through a type of macropinocytosis

independent of PI3K activity (Cortese et al. 2008). The roles of PI3K in macropinocytosis also vary in different cell types and with stimulation by different signals. Inhibitors of PI3K inhibit both membrane ruffling and macropinocytosis induced by insulin in epidermoid carcinoma KB cells (Kotani et al. 1995), but only inhibit macropinosome closure not membrane ruffling in EGF-stimulated epidermal A431 cells (Araki et al. 2007). Molecular and functional distinctions of these two types of macropinosomes remain to be characterized, and Neuro-2a may be an excellent system to study these vesicles due to its efficiency for transfection and the polarized nature of a neuronal cell line.

Despite the high degree of homology in amino acid sequence (Golomb et al. 2004), myosin IIA and -IIB have been shown to have differences in ATPase activities, contraction rates and subcellular localizations (Bresnick 1999). Myosin IIA and -IIB activities can be regulated by different signaling pathways and have distinct as well as overlapping functions (Murakami et al. 1998; Murakami et al. 1995; Sandquist et al. 2006). Myosin IIB was capable of partially compensating for the absence of myosin IIA in cell contractility but not in migration involved in cardiogenesis (Bao et al. 2007). Myosin IIA and IIB play different roles in cell migration, polarization and morphological change (Betapudi et al. 2006; Even-Ram et al. 2007; Swailes et al. 2006; Vicente-Manzanares et al. 2007). Myosin IIB directs cell migration by coordinating protrusive activity in the establishment and stabilization of cell polarity (Lo et al. 2004; Vicente-Manzanares et al. 2007). Myosin IIA has been implicated in the regulation of actin retrograde flow and controlling cell adhesion (Cai et al. 2006; Vicente-Manzanares et al. 2007). In mouse embryonic stem cells genetically ablated of myosin IIA, flattened cell shape, loss of focal adhesion, and increased cell migration have been reported (Even-Ram et al. 2007). Interestingly, an increase in membrane ruffles was shown in the myosin IIA-deficient cells attributed to stabilization of microtubules (Even-Ram et al. 2007), similarly as observed in our myosin IIA KD cells.

Here, we present another example in which myosin IIA and IIB appear to play distinct roles in macropinocytosis and membrane ruffle formation. By using ML-7 to inhibit myosin light-chain kinase, it has been previously shown that myosin II plays a role in phagocytosis and macropinocytosis in macrophages (Araki et al. 2003). However, specific roles of non-muscle myosin II isoforms in macropinocytosis have not been addressed. Different myosins may be employed for macropinocytosis in different species. In *Dictyostellium*, macropinocytosis is dependent on myosin I but not myosin II (Jung et al. 1996; Novak et al. 1995). Although expression of catalytically inactive myosin II or inhibition of myosin II by blebbistatin in *Dictyostellium* inhibited macropinocytosis, this was likely a result of formation of cytoplasmic aggregates of inactive myosin II (Shu et al. 2005). In our study, we characterized the roles of myosin II isoforms by using blebbistatin and myosin II isoform knockdown. Based on the observations that myosin IIB is rapidly relocalized to the sites of membrane ruffles in response to the stimulants and myosin IIB knockdown shows a significant reduction of membrane ruffle formation and macropinocytosis, myosin IIB appears to be a major player in membrane ruffle formation preceding macropinocytosis. However, more definitive role of myosin IIB in macropinocytosis in neuronal cells awaits future study possibly by using direct time-lapse imaging, immuno-EM and analysis of various myosin IIB mutants. Unexpectedly, myosin IIA knockdown has an opposite effect on membrane ruffle formation and macropinocytosis. In the double knockdown cells targeting both myosin IIA and IIB, macropinocytosis was reduced down to the level of myosin IIB knockdown alone. Although the underlying mechanism is presently unclear, it is possible that the myosin IIA and IIB impinge on the same molecular pathway involved in macropinocytosis. The increase in macropinocytosis in the myosin IIA knockdown cells is possibly due to an increase in myosin IIB-mediated activities.

Membrane ruffling is long known to be a prerequisite of macropinocytosis. Ruffles may recede without the formation of macropinosomes, but may also fold back to the plasma membrane which subsequently closes into vesicles (Swanson 2008; Swanson and Watts 1995). Two types of membrane ruffles have been observed in response to growth factors depending on their localizations relative to the leading edge of the cell: cell peripheral ruffles are wavy and at the edge of the cell, whereas dorsal ruffles tend to be circular and away from the leading edge (Suetsugu et al. 2003). In Neuro-2a cells, PMA-induced membrane ruffles were frequently wavy, on the neurites/processes, at the cell edge, thus resembling the peripheral ruffles. IGF-1-induced membrane ruffles were circular, on the cell bodies, away from the cell edge, similar to the dorsal ruffles. The distinction of dorsal vs. peripheral ruffles remains unclear; neither is known of the function of macropinocytosis induced by IGF-1 and PMA. We, however, have evidence that macropinocytosis in the axons of primary neurons plays a critical role in negative guidance factor-induced repulsive axon turning (Kolpak et al. 2009). With the establishment of Neuro-2a as a convenient system for studying macropinocytosis, future study will reveal the mechanisms and functions of macropinocytosis in cells such as neurons.

Material and Methods

Cell culture and transfection

Neuro-2a cells were maintained in 10% FBS in DMEM and cultured on poly-D-lysine-coated glass coverslips. Neuro-2a cells were seeded onto coverslips, and 16 hours after splitting, culture media was changed to serum-free media for 5–6 hours before stimultation with PMA or IGF-1.

For knockdown studies, Neuro-2a cells were transfected by Lipofectamine (Invitrogen) for 72 hours with 20 nM non-targeting siCONTROL (Dharmacon) or siRNA targeting nonmuscle myosin II heavy chain A or myosin II heavy chain B. Two sets of siRNA oligos were used to target *MHC-IIA* or *MHC-IIB* to ensure specificity of knockdown phenotypes. *MHC-IIA* gene was targeted by IIA1 siRNA (sense sequence: AUAAGAACCUGCCCAUCUAUU) and IIA2 siRNA (sense sequence: GGGCUUAUCUACACCUAUUUU). *MHC-IIB* gene was targeted by IIB1 siRNA (sense sequence: GGGCAUCUCUGCUCGCUAUUU) and IIB2 siRNA (sense sequence: GUAUUAAGUUUGCGAAGGAUU).

Dextran internalization

2.5 mg/ml 10K or 40K FITC-dextran (Molecular Probes) was used to assay macropinocytosis in Neuro-2a cultures. Cells were incubated with phorbol 12-myristate 13-acetate (PMA, from Sigma) for 3 min at 37°C prior to mixing in with the FITC-dextran. All dextran labeling was carried out for 2 min at 37°C. The effect of insulin like growth factor (IGF-1, Sigma) on dextran uptake was assayed by incubation of the cells with 50 ng/ml IGF-1 for 2 min and then mixing in with FITC-dextran to label for 2 min at 37°C. To study the effects of specific inhibitors on macropinocytosis, 100 μM (S)-(-)-Blebbistain (Toronto Research Chemicals), 100 μM 5-(N-ethyl-N-isopropyl) amirolide (EIPA) (Sigma) was used to pre-treat cells for 5–10 minutes before dextran uptake was assayed.

After labeling, cells were washed 3 times in DMEM and fixed in 4% paraformaldehyde. Fluorescence and DIC images of randomly chosen cells were acquired using a 63X Plan Apochromat objective on an inverted Zeiss Axiovert 200 microscope equipped with a digital camera (AxioCam MRm). The fluorescence images were taken at fixed exposure time for all samples to ensure that the large macropinosomes but not the small vesicles were clearly visible. The dextran+ (dex+) macropinosomes were determined by three criteria including

bright fluorescent labeling, large vesicle size (>0.2 um) and coincidence with reverse-shadowcast vesicles in DIC. The percentage of cells containing dex+ macropinosomes was scored from over 200 Neuro-2a cells for each sample and at least three sets of independent experiments were performed.

HRP uptake and quantification

2.5×10^5 Neuro-2a cells were cultured on the coverslips coated with 10 μg/ml poly D-lysine. After 16 hours of culture, cells were changed into serum-free media for 5 hours. Neuro-2a cells were labeled with 4 mg/ml horseradish peroxidase (HRP, Sigma) for 5 minutes with vehicle, PMA or IGF-1. The cells were rinsed 2 times with PBS and trypsinized for 3 minutes with 0.25% trypsin+1mM EDTA at room temperature followed by 20 minutes on ice until the cells were detached from the coverslips. Trypsinization was stopped by 1% BSA+1mM $MgCl_2$+1mM $CaCl_2$ in PBS for 5 minutes on ice. Cells were collected by centrifugation at 1200 rpm for 3 minutes at 4°C, and then washed with ice cold PBS for 2 times to remove trypsin. Cells were lysed in 80 μl buffer containing 0.1% Triton X-100 in PBS for 20 minutes on ice. The lysate was centrifuged at 12,000 rpm for 10 minutes at 4°C. 2 μl of supernatant was added to a 96-well plate and developed by a chemiluminescent substrate kit (SuperSignal ELISA Pico Chemiluminescent Substrate, Thermo Scientific, Rockford, IL), following the manufacturer's instruction. The luminescence was measured for 0.1 second at 425 nm wavelength by a Wallac EnVision 2102 Multilabel Reader (Perkin-Elmer).

Immunofluorescence staining

Neuro-2a cells were pretreated with 1 μM PMA for 3 minutes or 50ng/ml IGF-1 for 2 minutes, followed by labeling with FITC-dextran for 2 minutes and then fixed with cold 4% paraformaldehyde for 2 hours, washed with PBS for 3 times, permeabilized with 0.01% Triton X-100 for 1 min, washed with PBS for 3 times, and then blocked with 10% calf serum in PBS for 1 hour. Polyclonal antibodies specific for nonmuscle myosin II heavy chain A (MHC-A) and nonmuscle myosin II heavy chain B (MHC-B) were obtained from COVANCE and used at a dilution of 1:200. Incubation of primary antibodies was followed by incubation with Cy3-conjugated secondary antibody (1:400, Jackson ImmunoResearch).

For staining with Alexa 594-conjugated phalloidin, Neuro-2a cultures were fixed with 4% paraformaldehyde for 20 minutes, permeabilized with 0.1% Triton X-100 for 5 min, and then blocked with 1% BSA for 30 min. Alexa 594-conjugated phalloidin (Invitrogen) was diluted in PBS (1:40) and incubated for 1 hour at room temperature. Stained samples were photographed and actin-rich, wavy or circular membrane ruffles were classified based on their localizations to the neurites/processes or around the cell bodies. The percentage of cells containing each type of membrane ruffle was scored from over 120 cells total for each sample, and each experiment was repeated for 3 times.

Western blot analysis

For western blot experiments, Neuro-2a cells transfected with siRNA targeting myosin II isoforms, IIA1, IIA2, IIB1 or IIB2, were washed with ice-cold PBS and scraped in lysis buffer containing 20 mM Tris-HCl (pH 7.5), 1.2% Triton X-100, 0.1% 2-mercaptoethanol, 0.5 mM EDTA, and protease inhibitors (Sigma) for 20 min. Cell extracts were centrifuged at 13,000 rpm for 10 min at 4 °C and the supernatant was boiled in 5X reducing sample buffer for 5 min. 10 μg of proteins were loaded onto a 6.5% SDS-PAGE gel. Immunoblotting was performed by incubating with either MHC-A antibody (1:500 dilution), MHC-B antibody (1:000 dilution) or mouse anti-β-actin antibody (1:10,000, from Sigma), followed by incubation with peroxidase-conjugated secondary antibody (1:10,000, Jackson

ImmunoResearch) and finally detected using SuperSignal West Pico Chemiluminescent Substrate (Pierce).

Statistical Analysis

All data are expressed as mean ± s.e.m. Statistical analyses were performed using the Student's *t*-test and P values < 0.05 were considered to be statistically significant.

Acknowledgments

This work was supported by a grant from National Institutes of Health to Z. Z. Bao (EY014980) and an NIH predoctoral fellowship to A. L. Kolpak (FNS058170A). We thank Dr. Elizabeth Luna for helpful advice and discussions.

References

Aballay A, Stahl PD, Mayorga LS. Phorbol ester promotes endocytosis by activating a factor involved in endosome fusion. Journal of Cell Science. 1999; 112(Pt 15):2549–57. [PubMed: 10393811]

Amyere M, Payrastre B, Krause U, Van Der Smissen P, Veithen A, Courtoy PJ. Constitutive macropinocytosis in oncogene-transformed fibroblasts depends on sequential permanent activation of phosphoinositide 3-kinase and phospholipase C. Molecular Biology of the Cell. 2000; 11(10): 3453–67. [PubMed: 11029048]

Anton IM, Saville SP, Byrne MJ, Curcio C, Ramesh N, Hartwig JH, Geha RS. WIP participates in actin reorganization and ruffle formation induced by PDGF. Journal of Cell Science. 2003; 116(Pt 12):2443–51. [PubMed: 12724353]

Araki N, Egami Y, Watanabe Y, Hatae T. Phosphoinositide metabolism during membrane ruffling and macropinosome formation in EGF-stimulated A431 cells. Experimental Cell Research. 2007; 313(7):1496–507. [PubMed: 17368443]

Araki N, Hatae T, Furukawa A, Swanson JA. Phosphoinositide-3-kinase-independent contractile activities associated with Fcgamma-receptor-mediated phagocytosis and macropinocytosis in macrophages. Journal of Cell Science. 2003; 116(Pt 2):247–57. [PubMed: 12482911]

Araki N, Johnson MT, Swanson JA. A role for phosphoinositide 3-kinase in the completion of macropinocytosis and phagocytosis by macrophages. Journal of Cell Biology. 1996; 135(5):1249–60. [PubMed: 8947549]

Bao J, Ma X, Liu C, Adelstein RS. Replacement of nonmuscle myosin II-B with II-A rescues brain but not cardiac defects in mice. Journal of Biological Chemistry. 2007; 282(30):22102–11. [PubMed: 17519229]

Beron J, Forster I, Beguin P, Geering K, Verrey F. Phorbol 12-myristate 13-acetate down-regulates Na, K-ATPase independent of its protein kinase C site: decrease in basolateral cell surface area. Molecular Biology of the Cell. 1997; 8(3):387–98. [PubMed: 9188092]

Betapudi V, Licate LS, Egelhoff TT. Distinct roles of nonmuscle myosin II isoforms in the regulation of MDA-MB-231 breast cancer cell spreading and migration. Cancer Research. 2006; 66(9):4725–33. [PubMed: 16651425]

Bresnick AR. Molecular mechanisms of nonmuscle myosin-II regulation. Current Opinion in Cell Biology. 1999; 11(1):26–33. [PubMed: 10047526]

Cai Y, Biais N, Giannone G, Tanase M, Jiang G, Hofman JM, Wiggins CH, Silberzan P, Buguin A, Ladoux B, et al. Nonmuscle myosin IIA-dependent force inhibits cell spreading and drives F-actin flow. Biophysical Journal. 2006; 91(10):3907–20. [PubMed: 16920834]

Conner SD, Schmid SL. Regulated portals of entry into the cell. Nature. 2003; 422(6927):37–44. [PubMed: 12621426]

Conti MA, Adelstein RS. Nonmuscle myosin II moves in new directions. Journal of Cell Science. 2008; 121(Pt 1):11–8. [PubMed: 18096687]

Cortese K, Sahores M, Madsen CD, Tacchetti C, Blasi F. Clathrin and LRP-1-independent constitutive endocytosis and recycling of uPAR. PLoS ONE. 2008; 3(11):e3730. [Electronic Resource]. [PubMed: 19008962]

D'Angelo R, Aresta S, Blangy A, Del Maestro L, Louvard D, Arpin M. Interaction of ezrin with the novel guanine nucleotide exchange factor PLEKHG6 promotes RhoG-dependent apical cytoskeleton rearrangements in epithelial cells. Molecular Biology of the Cell. 2007; 18(12):4780–93. [PubMed: 17881735]

Deacon SW, Beeser A, Fukui JA, Rennefahrt UE, Myers C, Chernoff J, Peterson JR. An isoform-selective, small-molecule inhibitor targets the autoregulatory mechanism of p21-activated kinase. Chemistry & Biology. 2008; 15(4):322–31. [see comment]. [PubMed: 18420139]

Dharmawardhane S, Schurmann A, Sells MA, Chernoff J, Schmid SL, Bokoch GM. Regulation of macropinocytosis by p21-activated kinase-1. Molecular Biology of the Cell. 2000; 11(10):3341–52. [PubMed: 11029040]

Ellerbroek SM, Wennerberg K, Arthur WT, Dunty JM, Bowman DR, DeMali KA, Der C, Burridge K. SGEF, a RhoG guanine nucleotide exchange factor that stimulates macropinocytosis. Molecular Biology of the Cell. 2004; 15(7):3309–19. [PubMed: 15133129]

Even-Ram S, Doyle AD, Conti MA, Matsumoto K, Adelstein RS, Yamada KM. Myosin IIA regulates cell motility and actomyosin-microtubule crosstalk. Nature Cell Biology. 2007; 9(3):299–309. [erratum appears in Nat Cell Biol. 2007 Apr;9(4):480].

Fiorentini C, Falzano L, Fabbri A, Stringaro A, Logozzi M, Travaglione S, Contamin S, Arancia G, Malorni W, Fais S. Activation of rho GTPases by cytotoxic necrotizing factor 1 induces macropinocytosis and scavenging activity in epithelial cells. Molecular Biology of the Cell. 2001; 12(7):2061–73. [PubMed: 11452003]

Golomb E, Ma X, Jana SS, Preston YA, Kawamoto S, Shoham NG, Goldin E, Conti MA, Sellers JR, Adelstein RS. Identification and characterization of nonmuscle myosin II-C, a new member of the myosin II family. Journal of Biological Chemistry. 2004; 279(4):2800–8. [PubMed: 14594953]

Hall A. Ras-related GTPases and the cytoskeleton. Molecular Biology of the Cell. 1992; 3(5):475–9. [PubMed: 1611153]

Hewlett LJ, Prescott AR, Watts C. The coated pit and macropinocytic pathways serve distinct endosome populations. Journal of Cell Biology. 1994; 124(5):689–703. [PubMed: 8120092]

Jones AT. Macropinocytosis: searching for an endocytic identity and role in the uptake of cell penetrating peptides. Journal of Cellular & Molecular Medicine. 2007; 11(4):670–84. [PubMed: 17760832]

Jung G, Wu X, Hammer JA 3rd. Dictyostelium mutants lacking multiple classic myosin I isoforms reveal combinations of shared and distinct functions. Journal of Cell Biology. 1996; 133(2):305–23. [see comment]. [PubMed: 8609164]

Kolpak A, Jiang J, Guo D, Standley C, Bellve K, Fogarty K, Bao ZZ. Negative guidance factor-induced macropinocytosis in the growth cone plays a critical role in repulsive axon turning. Journal of Neuroscience. 2009 In press.

Kotani K, Hara K, Kotani K, Yonezawa K, Kasuga M. Phosphoinositide 3-kinase as an upstream regulator of the small GTP-binding protein Rac in the insulin signaling of membrane ruffling. Biochemical & Biophysical Research Communications. 1995; 208(3):985–90. [PubMed: 7702629]

Kruth HS, Huang W, Ishii I, Zhang WY. Macrophage foam cell formation with native low density lipoprotein. Journal of Biological Chemistry. 2002; 277(37):34573–80. [PubMed: 12118008]

Kruth HS, Jones NL, Huang W, Zhao B, Ishii I, Chang J, Combs CA, Malide D, Zhang WY. Macropinocytosis is the endocytic pathway that mediates macrophage foam cell formation with native low density lipoprotein. Journal of Biological Chemistry. 2005; 280(3):2352–60. [PubMed: 15533943]

Landsverk ML, Epstein HF. Genetic analysis of myosin II assembly and organization in model organisms. Cellular & Molecular Life Sciences. 2005; 62(19–20):2270–82. [PubMed: 16142426]

Langweiler M, Davis BH. Comparative study of assays for stimulated fluid pinocytosis in canine and human neutrophils. American Journal of Veterinary Research. 1988; 49(5):663–6. [PubMed: 3395011]

Lo CM, Buxton DB, Chua GC, Dembo M, Adelstein RS, Wang YL. Nonmuscle myosin IIb is involved in the guidance of fibroblast migration. Molecular Biology of the Cell. 2004; 15(3):982–9. [PubMed: 14699073]

Maniak M. Fluid-phase uptake and transit in axenic Dictyostelium cells. Biochimica et Biophysica Acta. 2001; 1525(3):197–204. [PubMed: 11257433]

Meier O, Boucke K, Hammer SV, Keller S, Stidwill RP, Hemmi S, Greber UF. Adenovirus triggers macropinocytosis and endosomal leakage together with its clathrin-mediated uptake. Journal of Cell Biology. 2002; 158(6):1119–31. [PubMed: 12221069]

Meier O, Greber UF. Adenovirus endocytosis. Journal of Gene Medicine. 2004; 6 Suppl 1:S152–63. [PubMed: 14978758]

Murakami N, Chauhan VP, Elzinga M. Two nonmuscle myosin II heavy chain isoforms expressed in rabbit brains: filament forming properties, the effects of phosphorylation by protein kinase C and casein kinase II, and location of the phosphorylation sites. Biochemistry. 1998; 37(7):1989–2003. [PubMed: 9485326]

Murakami N, Singh SS, Chauhan VP, Elzinga M. Phospholipid binding, phosphorylation by protein kinase C, and filament assembly of the COOH terminal heavy chain fragments of nonmuscle myosin II isoforms MIIA and MIIB. Biochemistry. 1995; 34(49):16046–55. [PubMed: 8519761]

Nobes C, Marsh M. Dendritic cells: new roles for Cdc42 and Rac in antigen uptake? Current Biology. 2000; 10(20):R739–41. [PubMed: 11069097]

Norbury CC. Drinking a lot is good for dendritic cells. Immunology. 2006; 117(4):443–51. [PubMed: 16556257]

Norbury CC, Hewlett LJ, Prescott AR, Shastri N, Watts C. Class I MHC presentation of exogenous soluble antigen via macropinocytosis in bone marrow macrophages. Immunity. 1995; 3(6):783–91. [PubMed: 8777723]

Novak KD, Peterson MD, Reedy MC, Titus MA. Dictyostelium myosin I double mutants exhibit conditional defects in pinocytosis. Journal of Cell Biology. 1995; 131(5):1205–21. [PubMed: 8522584]

Pelkmans L, Helenius A. Insider information: what viruses tell us about endocytosis. Current Opinion in Cell Biology. 2003; 15(4):414–22. [PubMed: 12892781]

Phaire-Washington L, Wang E, Silverstein SC. Phorbol myristate acetate stimulates pinocytosis and membrane spreading in mouse peritoneal macrophages. Journal of Cell Biology. 1980; 86(2):634–40. [PubMed: 7400219]

Racoosin EL, Swanson JA. Macropinosome maturation and fusion with tubular lysosomes in macrophages. Journal of Cell Biology. 1993; 121(5):1011–20. [PubMed: 8099075]

Rupper A, Lee K, Knecht D, Cardelli J. Sequential activities of phosphoinositide 3-kinase, PKB/Aakt, and Rab7 during macropinosome formation in Dictyostelium. Molecular Biology of the Cell. 2001; 12(9):2813–24. [PubMed: 11553719]

Sandquist JC, Swenson KI, Demali KA, Burridge K, Means AR. Rho kinase differentially regulates phosphorylation of nonmuscle myosin II isoforms A and B during cell rounding and migration. Journal of Biological Chemistry. 2006; 281(47):35873–83. [PubMed: 17020881]

Sato SB, Kiyosue K, Taguchi T, Kasai M, Toyama S. Okadaic acid gives concentration-dependent reciprocal effects on the fluid phase endocytosis activated by Ca2+ and phorbol 12-myristate 13-acetate. Journal of Cellular Physiology. 1996; 166(1):66–75. [PubMed: 8557777]

Shu S, Liu X, Korn ED. Blebbistatin and blebbistatin-inactivated myosin II inhibit myosin II-independent processes in Dictyostelium. Proceedings of the National Academy of Sciences of the United States of America. 2005; 102(5):1472–7. [PubMed: 15671182]

Sieczkarski SB, Whittaker GR. Dissecting virus entry via endocytosis. Journal of General Virology. 2002; 83(Pt 7):1535–45. [PubMed: 12075072]

Suetsugu S, Yamazaki D, Kurisu S, Takenawa T. Differential roles of WAVE1 and WAVE2 in dorsal and peripheral ruffle formation for fibroblast cell migration. Developmental Cell. 2003; 5(4):595–609. [PubMed: 14536061]

Swailes NT, Colegrave M, Knight PJ, Peckham M. Non-muscle myosins 2A and 2B drive changes in cell morphology that occur as myoblasts align and fuse. Journal of Cell Science. 2006; 119(Pt 17): 3561–70. [PubMed: 16895968]

Swanson JA. Shaping cups into phagosomes and macropinosomes. Nature Reviews Molecular Cell Biology. 2008; 9(8):639–49.

Swanson JA, Watts C. Macropincytosis. Trends Cell Biol. 1995; 5(11):424–8. [PubMed: 14732047]

Vicente-Manzanares M, Zareno J, Whitmore L, Choi CK, Horwitz AF. Regulation of protrusion, adhesion dynamics, and polarity by myosins IIA and IIB in migrating cells. Journal of Cell Biology. 2007; 176(5):573–80. [erratum appears in J Cell Biol. 2007 Mar 26;176(7):1073]. [PubMed: 17312025]

West MA, Bretscher MS, Watts C. Distinct endocytotic pathways in epidermal growth factor-stimulated human carcinoma A431 cells. Journal of Cell Biology. 1989; 109(6 Pt 1):2731–9. [erratum appears in J Cell Biol 1990 Mar;110(3):859]. [PubMed: 2556406]

West MA, Prescott AR, Eskelinen EL, Ridley AJ, Watts C. Rac is required for constitutive macropinocytosis by dendritic cells but does not control its downregulation. Current Biology. 2000; 10(14):839–48. [PubMed: 10899002]

Wylie SR, Chantler PD. Separate but linked functions of conventional myosins modulate adhesion and neurite outgrowth. Nature Cell Biology. 2001; 3(1):88–92.

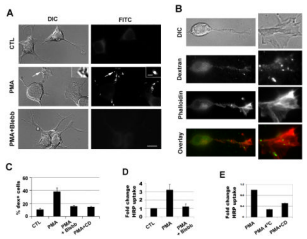

Figure 1.

PMA-induced macropinocytosis in Neuro-2a cells is inhibited by blebbistatin. (A) Neuro-2a cells were pre-treated with PMA for 3 minutes, followed by labeling with FITC-dextran for 2 minutes and the cells were subsequently rinsed and fixed. Labeling of dextran was examined by fluorescence microscopy and the localization in the reverse shadowcast vesicles was confirmed by DIC image. Preincubation with blebbistatin for 5 minutes before addition of PMA and FITC-dextran inhibited macropinocytosis. (B) Dextran uptake was carried out with PMA. Cells were washed and stained with phalloidin to visualize F-actin. Note that dex+ vesicles were localized in the neurites around the actin-rich membrane ruffles. 3X magnification of the images are shown to the right. (C) Percentages of dextran-positive cells were scored from >200 cells in each experiment and at least three independent experiments were carried out. (D, E) Horseradish peroxidase (HRP) uptake was also used to measure macropinocytosis with addition of vehicle control, PMA, or PMA with inhibitors. Blebb: blebbistatin; CD: cytochalasin D. Scale bar=10μm; scale bar in inset=1 μm.

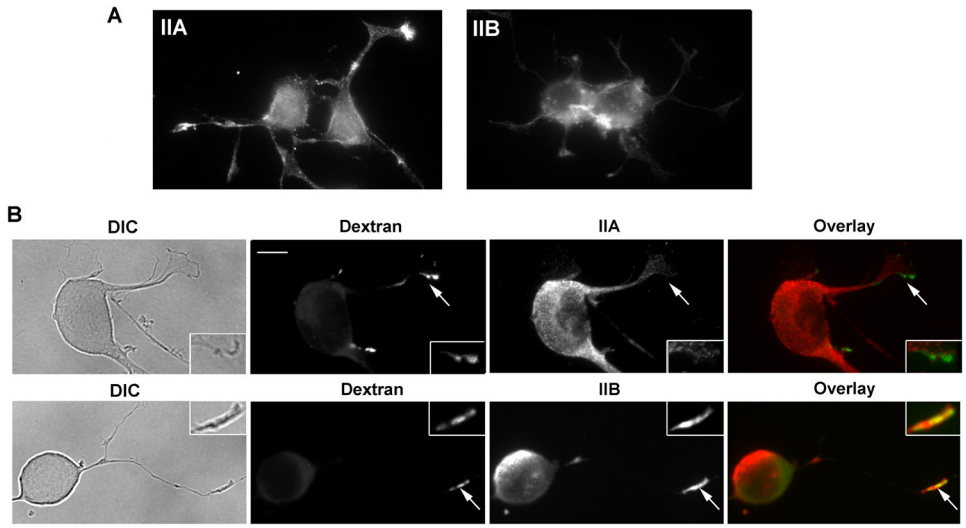

Figure 2.

Myosin IIB appears to localize in the same area with the newly formed dex+ vesicles induced by PMA in the growth cone of the neurites. (A) Untreated Neuro-2a cells were stained by antibodies against myosin IIA and IIB isoforms. Note that IIA is concentrated in the growth cones of the neurites whereas IIB is localized more in the cell body. (B) Neuro-2a cells were pre-treated with PMA for 3 minutes and then labeled with FITC-dextran for 2 minutes, rinsed and fixed. The cells were then immunostained with antibodies specific to myosin-IIA and IIB. Myosin IIA appears to concentrate in the cell body with only low amount present in the tips of the neurites. In contrast, myosin IIB appeared to be concentrated in the growth cones adjacent to the dex+ vesicles, in addition to its localization in the cell bodies. Scale bar=10 μm; 2× magnification shown in insets.

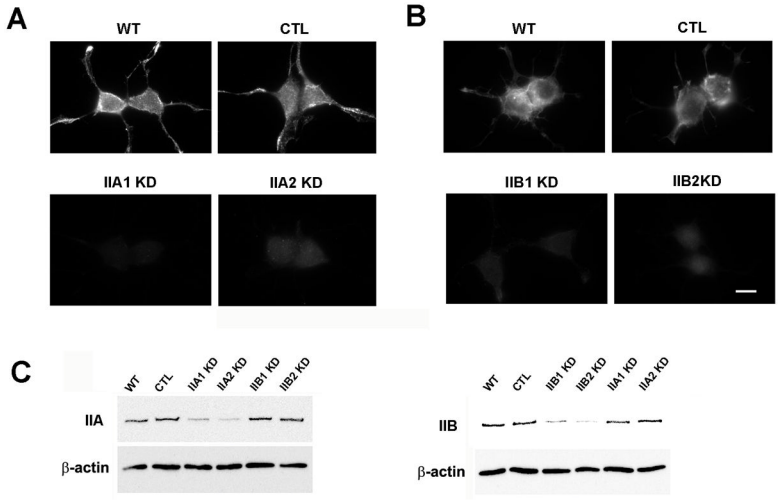

Figure 3.

Two sets of siRNAs each were used to knock down the expression of myosin IIA (IIA1 and IIA2) and IIB (IIB1 and IIB2) specifically. A non-silencing siRNA was transfected to use as a control (CTL). (A, B) The levels of myosin IIA and IIB proteins were analyzed at 72 hours after transfection of siRNA by immunofluorescent staining using antibodies against myosin IIA (A) and myosin IIB (B). (C) Decrease of myosin II proteins in the cells transfected with the siRNAs was also confirmed by western blot of cell extracts at 72 hours post-transfection. An antibody against β-actin was used as loading control. Scale bar=10 μm.

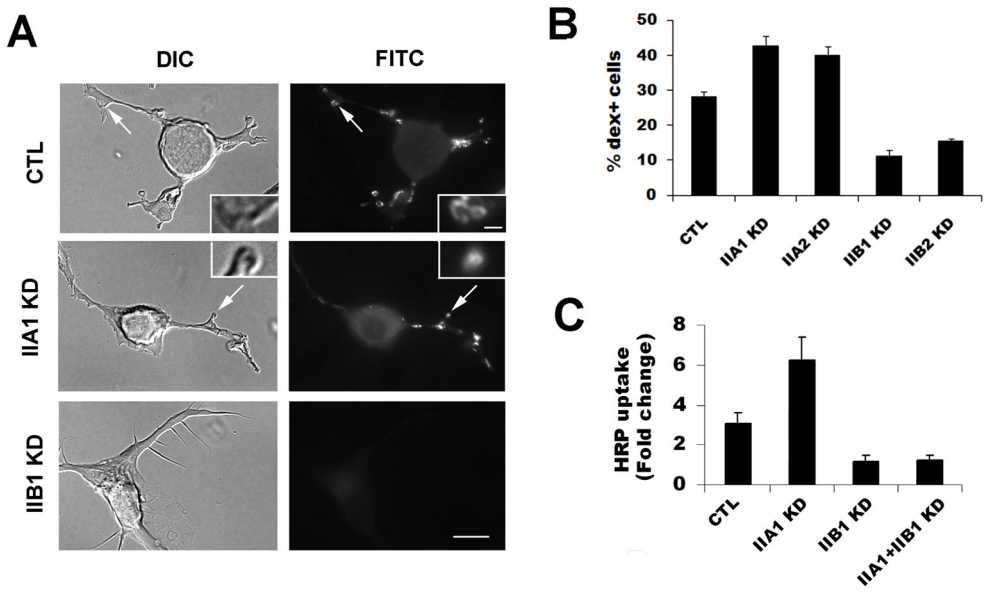

Figure 4.

Myosin IIA and -*IIB* knock-downs have distinct effects on PMA-induced macropinocytosis. (A) Neuro-2a cells were transfected with non-silencing control (CTL) or siRNA targeting *myosin IIA* (IIA1 and IIA2) or *myosin II*B (IIB1 and IIB2). FITC-dextran was added with PMA for 2 minutes to assay the formation of macropinoctyosis and the percentage of cells containing dex+ macropinosomes were quantified. (B) Myosin IIB knockdown cells (IIB1 KD and IIB2 KD) show a significant decrease in dex+ cells whereas myosin IIA-knockdown cells (IIA1 KD and IIA2 KD) show a significant increase in dextran uptake. (C) Horseradish peroxidase (HRP) was also used to measure macropinosome formation in the cells transfected with CTL, or IIA1 or IIB1 or co-transfected with both IIA1 and IIB1. Data were normalized to the level of HRP uptake of the unstimulated control cells included in each experiment. HRP uptake was significantly increased in IIA1 KD cells but reduced in IIB1 KD or IIA1/IIB1 double knockdown cells. Scale bar=10 μm; scale bar in inset=1 μm.

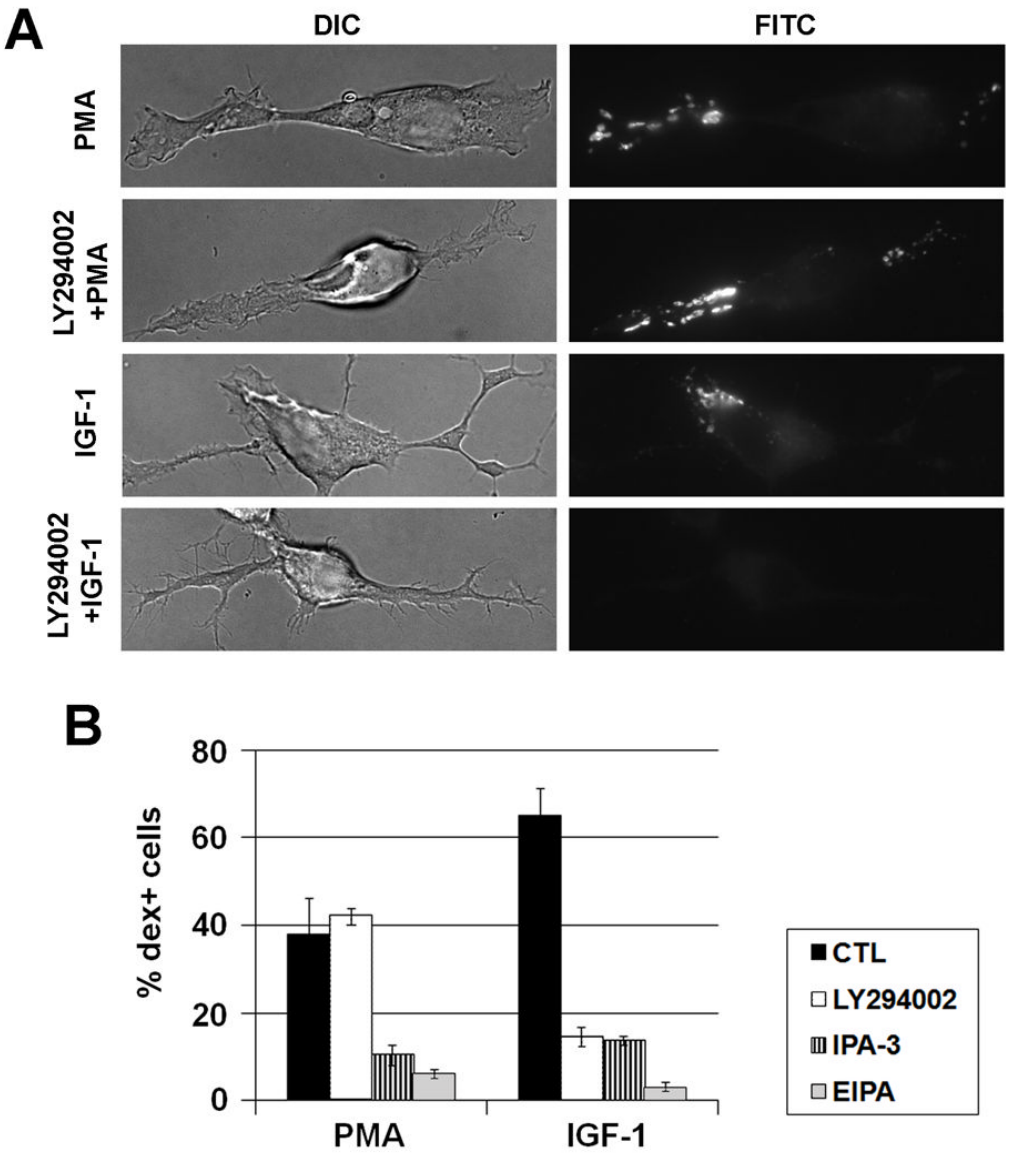

Figure 5.

Comparison of macropocytosis induced by PMA and IGF-1 in Neuro-2a cells. **A.** Macropinocytosis was induced by PMA or IGF-1 as shown by 2 minute-dextran labeling. Note that the PMA-induced macropinosomes are located more in the neurites or processes whereas the IGF-1-induced macropinosomes are located in the membrane ruffles close to the cell body. The role of PI3K in macropinocytosis was analyzed by pretreatment with a PI3K inhibitor LY294002 for 30 minutes, prior to addition of IGF-1 or PMA. **B.** Percentages of dex+ cells induced by PMA or IGF-1 were quantified, in the presence of vehicle control, 50 μM LY294002, 10 μM PAK-1 inhibitor (IPA-3), or 100μM EIPA. Note that IPA-3 and EIPA inhibited both PMA and IGF-1-induced macropinocytosis whereas LY294002 inhibited only IGF-1-induced macropinocytosis.

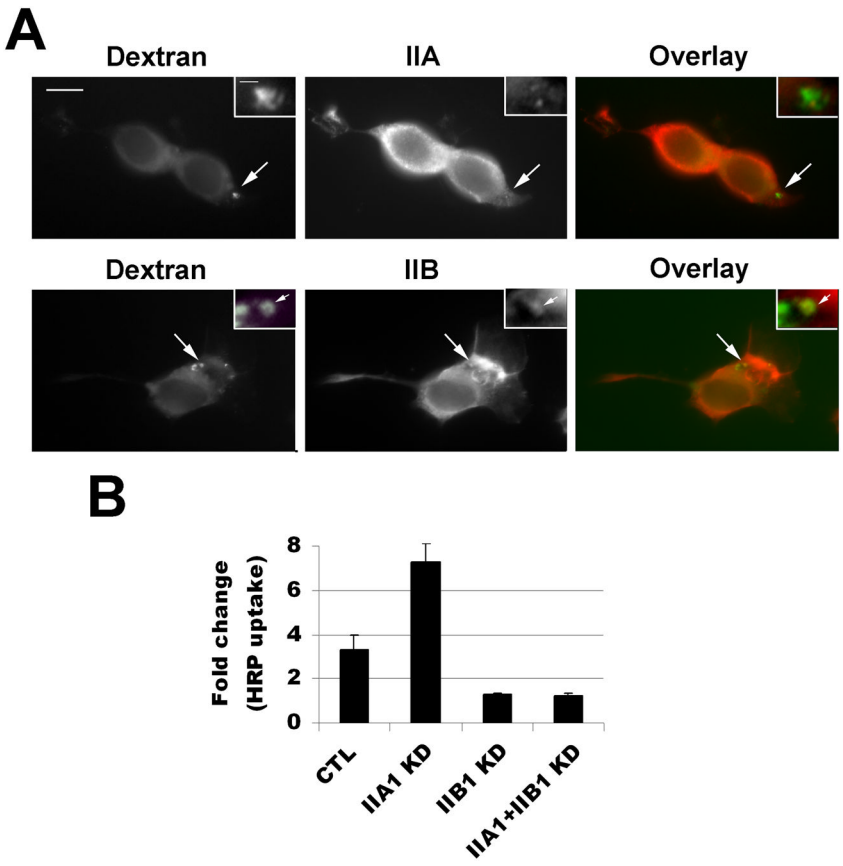

Figure 6.

Knock-down of myosin IIA and IIB showed opposite effects on macropinocytosis induced by IGF-1. (A) IGF-1 rapidly induced macropinocytosis in the Neuro-2a cells, more around the cell bodies than on the neurites. Myosin IIB appeared to localize in the areas of membrane ruffles whereas myosin IIA was more concentrated around the nucleus and neurites. (B) HRP uptake was performed on the cells transfected with CTL, IIA1, IIB1 or cotransfected with IIA1 and IIB1 siRNAs. IIB1 KD as well as IIA1+IIB1 KD cells showed diminished HRP uptake. In contrast, IIA1 KD cells exhibited a significant increase in HRP uptake. Scale bar=10 μm; 4× magnification shown in inset.

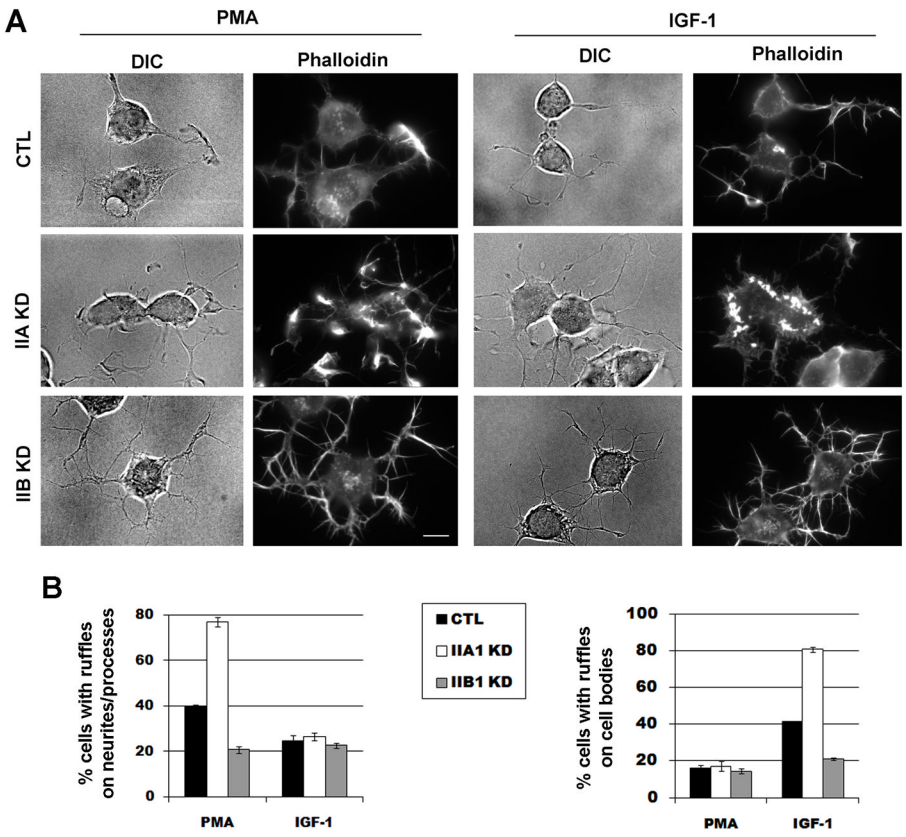

Figure 7.

Membrane ruffles were analyzed in the myosin II isoform knock-down cells in response to PMA or IGF-1. (A) Neuro-2a cells transfected with CTL, IIA KD or IIB KD were treated with either PMA for 3 minutes or IGF-1 for 2 minutes. Cells were rinsed, fixed and stained for actin filaments with Cy3-conjugated Phalloidin. PMA-induced membrane ruffles were predominantly localized on neurites/processes, whereas IGF-1-induced membrane ruffles were found around cell bodies. (B) Percentages of cells transfected with CTL, IIA KD or IIB KD were scored based on the presence of membrane ruffles on neurites/processes or cell bodies, in response to PMA or IGF-1. Note that IIA KD cells exhibited an increase in membrane ruffles. In contrast, IIB KD cells showed a decrease in membrane ruffles.